Study of Mg–Al–Ca magnesium alloy ameliorated with designed Al8Mn4Gd phase

Chaosheng Ma, Wenbo Yu, Xufeng Pi, Antoine Guitton

ARTICLE IN PRESS
JID: JMAA [m5+;September 22, 2020;9:52]

Available online at www.sciencedirect.com

ScienceDirect

Journal of Magnesium and Alloys xxx (xxxx) xxx

www.elsevier.com/locate/jma

Review

Study of Mg–Al–Ca magnesium alloy ameliorated with designed Al_8Mn_4Gd phase

Chaosheng Ma[a], Wenbo Yu[a,*], Xufeng Pi[a], Antoine Guitton[b,c]

[a] *School of Mechanical and Electronic Control Engineering, Beijing JiaoTong University, Beijing, China*
[b] *Université de Lorraine – CNRS – Arts et Métiers ParisTech – LEM3, F-57000 Metz, France*
[c] *Laboratory of Excellence on Design of Alloy Metals for low-mAss Structures (DAMAS), Université de Lorraine, F-57073 Metz, France*

Received 28 April 2020; received in revised form 27 July 2020; accepted 4 August 2020
Available online xxx

Abstract

To investigate the effect of Al_8Mn_4Gd phase on microstructural and mechanical properties of Mg–Al–Ca magnesium alloy, two Mg–2.5Al_2Ca and Mg–2.5Al_2Ca-0.1Al_8Mn_4Gd alloys were designed and compared in this work. The results show that a small amount of Gd can significantly refine α-Mg grains and change the morphology of Al_2Ca particles. Indeed, the formed Al_8Mn_4Gd phase could serve as a heterogeneous nucleation site for the α-Mg grains and Al_2Ca particles. Furthermore, the introduction of Gd not only optimized the mechanical properties of Mg–Al–Ca alloy, but also facilitated the thermal deformation (such as hot rolling).

Keywords: Mg–Al–Ca alloy; Al_8Mn_4Gd phase; Microstructure and mechanical properties; Hot rolling.

1. Introduction

Magnesium alloy castings have a great advantage in vehicle light-weighting, and aerospace engineering due to the low density, short processing cycle and assembly costs, which have attracted numerous studies [1–8]. As AZ series of magnesium alloy exhibits soften behavior at elevated temperature, Mg–Al–Ca alloys was developed to evaluate the mechanical properties due to the low price, texture weakening and good ignition resistance [9–11]. However, the poor plastic deformation ability and mechanical properties of as-cast Mg–Al–Ca alloys are challenges still to be addressed yet.

In cast Mg–Al–Ca alloys, the typical microstructure contains two phases: α-Mg grains and β-Al_2Ca[12]. Consequently, the most effective way to improve mechanical properties of Mg–Al–Ca based alloy is to modify β-Al_2Ca by alloying with Mn, Zn, Si, Sr and Rare Earth (RE) elements, etc. [13–16]. The modification mechanism is that the new formed particles could provide the nucleation site for the second phase. To fulfill this step, the particle should firstly form and exhibit one good crystallographic match with the second phase during solidification. For example, Li et al. [17] reported that introduction of manganese (Mn) into the as-cast Mg-5.5Al-3Ca wt.% alloys resulted in the formation of Al_8Mn_5 phase and increased the yield strength of the alloy from 366 MPa to 402 MPa. However, Mn addition has no refining effect on the microstructure of the as-cast alloys. Nakata et al. [18] reported that only 1% of Zn addition could significantly improve both strength and ductility of rolled Mg-8Al-1Ca-0.3Mn (AX81) alloy sheet. This is because that introduction of Zn facilitated the formation of homogeneous grain structure and isotropic basal texture. Son et al. [19] found that samarium (Sm) addition resulted in a microstructure composed of equiaxed and refined grains and grain sizes in Mg-5 wt%Al-3 wt% Ca-based alloys.

Recently, Li et al. [20] found that the formation of Al_8Mn_4Gd phase in AZ91 alloy could significantly refine

* Corresponding author.
E-mail address: wbyu@bjtu.edu.cn (W. Yu).

https://doi.org/10.1016/j.jma.2020.08.009

Table 1
Nominal composition of experimental alloys (wt.%).

Experimental alloys	Mg	Al	Mn	Ca	Gd
Mg-2.5Al_2Ca-0Al_8Mn_4Gd	90.533	5.433		4.035	
Mg-2.5Al_2Ca-0.1Al_8Mn_4Gd	88.276	6.232	0.875	3.99	0.626

α-Mg grains and $Mg_{17}Al_{12}$ particles, as Al_8Mn_4Gd phase can act as the heterogeneous nucleation site. However, so far, there are few reports about the effect of Al_8Mn_4Gd phase in Mg–Al–Ca alloy. Therefore, in the present work, two Mg-2.5Al_2Ca and Mg-2.5Al_2Ca-0.1Al_8Mn_4Gd alloys were designed and compared for investigating the effect of Al_8Mn_4Gd phase on microstructural and mechanical properties of Mg–Al–Ca magnesium alloy.

2. Experimental procedure

The mold and all tools of gravity casting were firstly pre-heated up to 250 °C for removing the moisture. The electric resistance furnace was used to melt 1 kg pure Mg and Al together in a steel crucible protected under the protection a mixture gas of CO_2 and SF_6, pure Mg and Al were heated to be melt in one electric resistance furnace. Subsequently, $MgGd_{30}$ and MgMn was used as master alloys for introducing Gd and Mn element. Then Ca was introduced through $CaAl_{20}$ master alloys. The melt was continuously held and stirred at 720 °C for 20 min after complete melting, homogeneous melt Mg-2.5Al_2Ca-0.1Al_8Mn_4Gd alloy was finally obtained and was poured into a pre-heated steel mold at 250 °C. The nominal composition of experimental alloys was given in Table 1.

Samples for observation were ground with silicon carbide and then successively polished with 6 μm, 3 μm, 1 μm and 0.25 μm diamond suspensions. To avoid the work-hardening caused by conventional grinding, a chemo-mechanical polishing was performed using Al_2O_3 (particle size: 0.04 μm) suspension. A diluted acetic acid solution comprising 50 mL distilled water, 150 mL anhydrous ethyl alcohol and 1 mL glacial acetic acid was used to etch the specimen surface. Scanning Electron Microscope (SEM) observation (Zeiss Merlin Germany) and X-Ray Diffraction (XRD) using Bruker D8 diffractometer (Karlsruhe, Germany) with Cu-Kα radiation were adopted to perform the microstructural observation and phase identification.

Tensile test was performed on a universal servo-hydraulic mechanical testing machine (Instron 5600, Norwood, MA) equipped with a knife-edge extensometer with a strain rate of 1 mm/min at room temperature in air. The samples were fabricated following GB/T228.1–2010 flat specimen standard. The dimensions were 85 mm in overall length and 35 mm in gauge length, 25 mm width and 15 mm in thickness. Each test was repeated six times for each composite in order to evaluate the corresponding mechanical properties.

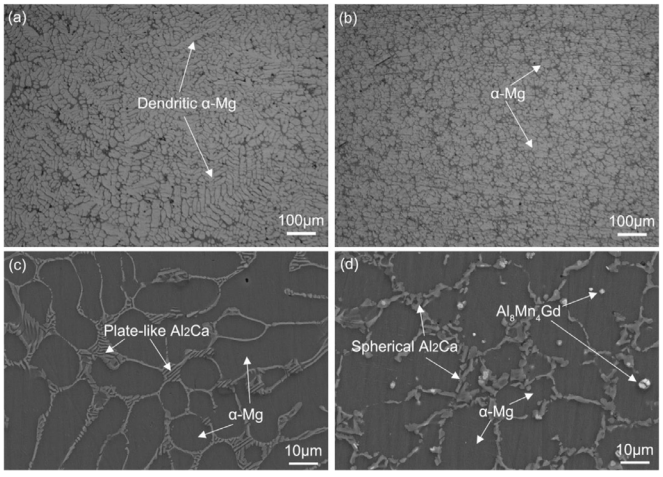

Fig. 1. Optical (top) and SEM (below) Morphologies of as-cast MgAlCa-0Gd (left) and Mg–Al–Ca-0.1Gd (right) alloys.

3. Results

3.1. Microstructural morphology and refine mechanism

The morphology and distribution of the particles in as-cast alloys were respectively observed by optical and SEM micrographs, as shown in Fig. 1, it is clear that Mg–Al–Ca alloy exhibit typical dendritic structure. (Fig. 1a). A lot of gray plate particles (Al_2Ca phase confirmed in Fig. 2) are found around the α-Mg dendrites and in α-Mg inter-dendrites (Fig. 1c). When Gd was added into Mg–Al–Ca alloy, the dendritic degree of α-Mg strongly decreased (Fig. 1b). Fig. 1d shows that the plate-like Al_2Ca changed into the spherical form and a new phase Al_8Mn_4Gd formed. It is confirmed by XRD shown in Fig. 2a.

As found from XRD result given in Fig. 2a, only α-Mg and Al_2Ca two phases were detected in Mg–Al–Ca alloy, while the new phase Al_8Mn_4Gd appeared when Gd was introduced into Mg–Al–Ca alloy. In addition, Fig. 2b shows the solidification paths of as-cast Mg-4Al_2Ca and Mg-0.5Al_8Mn_4Gd alloys calculated by Scheil model. It reveals that the Al_8Mn_4Gd phase precipitated at the temperature of 640 °C during the solidification process, while the precipitation of α-Mg and Al_2Ca phase starts below 600 °C.

As Al_8Mn_4Gd phase precipitated earlier than α-Mg and Al_2Ca phases, its ability of acting as potent nucleation sites for the α-Mg grains and Al_2Ca could be calculated by Bramfitt's equation shown in Eq. (1) [21], the degree of potency of the nucleation catalysts based on the average disregistries along low-index directions within low-index planes between

Please cite this article as: C. Ma, W. Yu, X. Pi et al., Study of Mg–Al–Ca magnesium alloy ameliorated with designed Al8Mn4Gd phase, Journal of Magnesium and Alloys, https://doi.org/10.1016/j.jma.2020.08.009

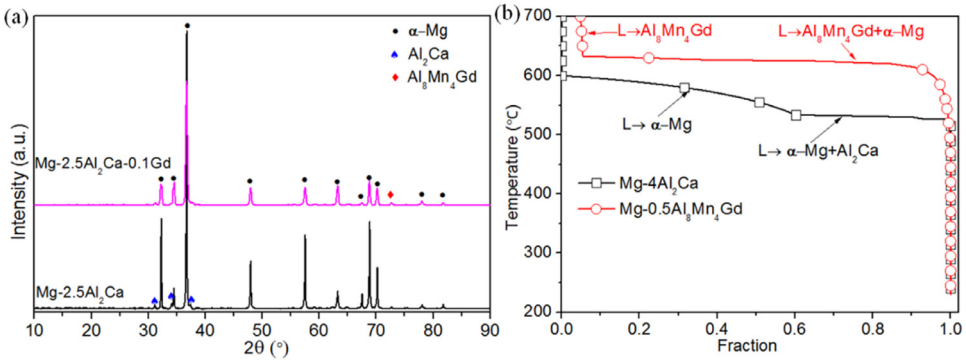

Fig. 2. (a) XRD patterns of as-cast MgAlCa-0Gd and MgAlCa-0.1Gd alloys (b) the solidification route calculated of Mg-4Al_2Ca and Mg-0.5Al_8Mn_4Gd alloys by JMatPro.

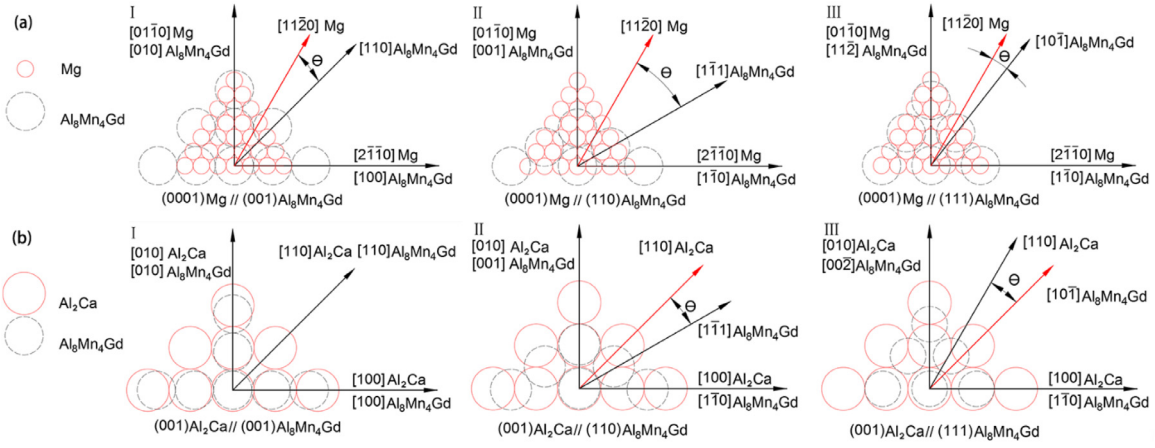

Fig. 3. Schematic plans of the crystallographic relationships:(a) between Mg and Al_8Mn_4Gd. (b) between Al_2Ca and Al_8Mn_4Gd.

substrate and nucleation solid.

$$\delta_{(hkl)n}^{(hkl)s} = \sum_{i}^{3}\left[(|d_{[uvw_s^i]}\cos\theta - d_{[uvw_n^i]}|/d_{[uvw_n^i]})/3\right] \times 100\% \quad (1)$$

Where $(hkl)_s$ is a low-index plane of substrate, $[uvw]_s$ is the low index direction in $(hkl)_s$, $d_{[uvw]s}$ is the interatomic spacing along $[uvw]_s$, $(hkl)_n$ is a low-index plane in the nucleation solid, $[uvw]_n$ is the low-index direction in $(hkl)_n$, $d[uvw]_n$ is the interatomic spacing along $[uvw]_n$, and θ is the angle between $[uvw]_s$ and $[uvw]_n$. If the disregistry δ of lattice spacing is less than 15%, the substrate can promote the nucleation of melt material. Mg is hexagonal structure with the lattice parameters of $a = 0.32093$ nm and $c = 0.52103$ nm. Al_8Mn_4Gd is tetragonal structure with the lattice parameters of $a = 0.8929$ nm and $c = 0.512$ nm. Al_2Ca is cubic structure with the lattice parameters of $a = 0.802$ nm.

Three low-index planes of Al_8Mn_4Gd, including (100), (110) and (111) were selected as matching planes. The (0001) plane of Mg and the (001) plane of Al_2Ca were used as nucleating plane. The schematic plans of the crystallographic relationships between Mg and Al_8Mn_4Gd, Al_2Ca and Al_8Mn_4Gd were shown in Fig. 3. By using the lattice parameters and Eq. (1), the disregistry between Mg and Al_8Mn_4Gd, Al_2Ca and Al_8Mn_4Gd were calculated and summarized in Tables 2 and 3. It was found that the mismatch was just 7% between $[1\bar{1}0]$ direction on the (111) plane of Al_8Mn_4Gd and $[2\bar{1}\bar{1}0]$ direction on the (0001) plane of Mg. Thus, Al_8Mn_4Gd can act as nucleation site to refine the α-Mg grains, which was also reported during the alloy solidification process [22–25]. Between Al_2Ca and Al_8Mn_4Gd, the calculation indicates that the mismatch was 0.113 (below 0.15) when the (110) plane of the Al_8Mn_4Gd was overlapped on the (001) plane of the Al_2Ca. Thus, the refining effect of Al_8Mn_4Gd on Al_2Ca as nucleation site is useful but not effective. This was consistent with the results shown in Fig. 1, the size of Al_2Ca phase only became a slightly smaller with the formation of Al_8Mn_4Gd phase. Moreover, the Al_2Ca lamellar located at the grain boundaries evolved into granular from with the formation of Al_8Mn_4Gd phase in Mg–Al–Ca alloy. Therefore, we confirmed that formation of Al_8Mn_4Gd phase could lead to efficiently refine α-Mg and change Al_2Ca phase morphologies, but the Al_2Ca phase was slightly refined.

3.2. Mechanical properties of as-cast and hot rolled

The room temperature stress-strain curves of the as-cast alloys and hot rolled ones are presented in Fig. 4. For the as-cast specimens, the addition of Gd into Mg-

Please cite this article as: C. Ma, W. Yu, X. Pi et al., Study of Mg–Al–Ca magnesium alloy ameliorated with designed Al8Mn4Gd phase, Journal of Magnesium and Alloys, https://doi.org/10.1016/j.jma.2020.08.009

Table 2
The results of planar disregistries between Mg and Al_8Mn_4Gd.

α-Mg plane	Al_8Mn_4Gd plane	α-Mg orientation	Al_8Mn_4Gd orientation	Results	Average
(0001)	(001)	$[2\bar{1}\bar{1}0]$	[100]	0.22	0.27
		$[11\bar{2}0]$	[110]	0.20	
		$[01\bar{1}0]$	[010]	0.39	
(0001)	(110)	$[2\bar{1}\bar{1}0]$	$[1\bar{1}0]$	0.07	0.16
		$[11\bar{2}0]$	$[1\bar{1}1]$	0.32	
		$[01\bar{1}0]$	[001]	0.08	
(0001)	(111)	$[2\bar{1}\bar{1}0]$	$[1\bar{1}0]$	0.07	0.11
		$[11\bar{2}0]$	$[10\bar{1}]$	0.18	
		$[01\bar{1}0]$	$[11\bar{2}]$	0.08	

Table 3
The results of planar disregistries between Al_2Ca and Al_8Mn_4Gd.

Al_2Ca plane	Al_8Mn_4Gd plane	Al_2Ca orientation	Al_8Mn_4Gd orientation	Results	Average
(001)	(001)	[100]	[100]	0.113	0.11
		[110]	[110]	0.113	
		[010]	[010]	0.113	
(001)	(110)	[100]	$[1\bar{1}0]$	0.575	0.319
		[110]	$[1\bar{1}1]$	0.107	
		[010]	[001]	0.277	
(001)	(111)	[100]	$[1\bar{1}0]$	0.575	0.229
		[110]	$[10\bar{1}]$	0.10	
		[010]	$[11\bar{2}]$	0.014	

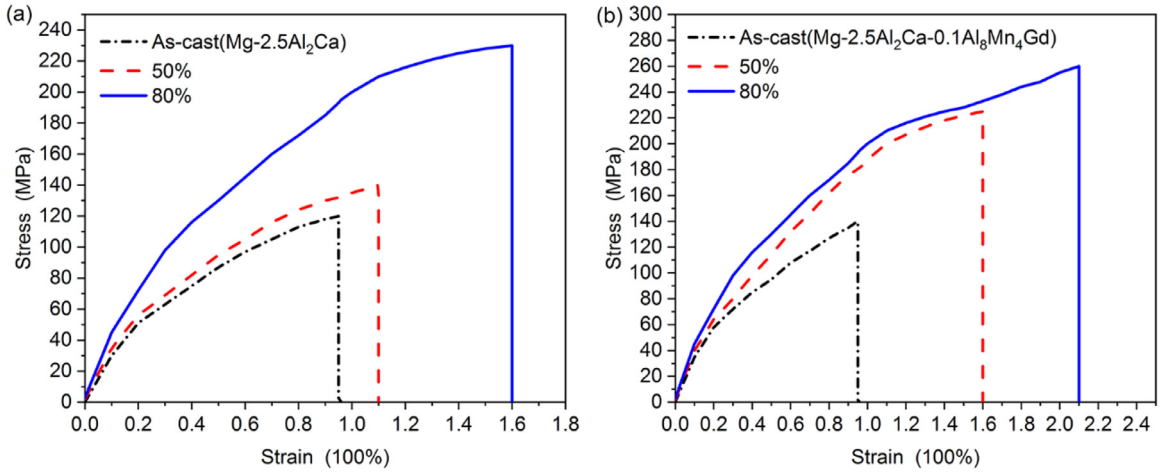

Fig. 4. Tensile stress-strain curve of as-cast and hot rolled specimens (a) Mg-2.5Al_2Ca alloy and (b) Mg-2.5Al_2Ca-0.1Al_8Mn_4Gd alloy.

2.5Al_2Ca alloy only has one weak improvement on the tensile strength and ductility. However, Mg-2.5Al_2Ca and Mg-2.5Al_2Ca-0.1Al_8Mn_4Gd alloys exhibit obvious different improvement in mechanical properties with hot rolling deformation. With 50% hot-roll deformation degree, the Ultimate Tensile Strength (UTS) and ductility of as-cast Mg-2.5Al_2Ca-0.1Al_8Mn_4Gd alloy were remarkably enhanced from 140 MPa and 1.1% to be 225 MPa and 1.6%. With further deformation to be 80% degree, UTS and ductility of Mg-2.5Al_2Ca-0.1Al_8Mn_4Gd alloy could reach 260 MPa and 2.1%. In contrast, the UTS and strain of Mg-2.5Al_2Ca were only enhanced from 119 MPa and 0.95% to be 140 MPa and 1.1% with 50% hot-roll deformation degree. Subsequently, different from the continuous improvement found in hot rolled 2.5Al_2Ca-0.1Al_8Mn_4Gd alloy, the UTS and strain of Mg-2.5Al_2Ca alloy suddenly jumped to 230 MPa and 1.6% with 80% deformation degree, even though these values are still lower than those of deformed Mg-2.5Al_2Ca-0.1Al_8Mn_4Gd.

Fig. 5 presents the microstructural morphologies of hot rolled two alloys with different degree of hot rolling deformation treatment. It is evident that both two alloys exhibit different Al_2Ca distribution. Even after hot rolling with 50% deformation degree, the lamellar Al_2Ca phase still accumulated with one necklace form in Mg-2.5Al_2Ca alloy. In contrast, Al_2Ca and Al_8Mn_4Gd phases already uniformly dispersed in Mg-2.5Al_2Ca-0.1Al_8Mn_4Gd alloy. When the deformation degree of specimens reached 80%, the lamellar Al_2Ca phase was almost broken and well distributed in Mg-2.5Al_2Ca alloy. Herein, one jump in mechanical properties occurred in hot rolled Mg-2.5Al_2Ca alloy from 50% to 80% deforma-

Please cite this article as: C. Ma, W. Yu, X. Pi et al., Study of Mg–Al–Ca magnesium alloy ameliorated with designed Al8Mn4Gd phase, Journal of Magnesium and Alloys, https://doi.org/10.1016/j.jma.2020.08.009

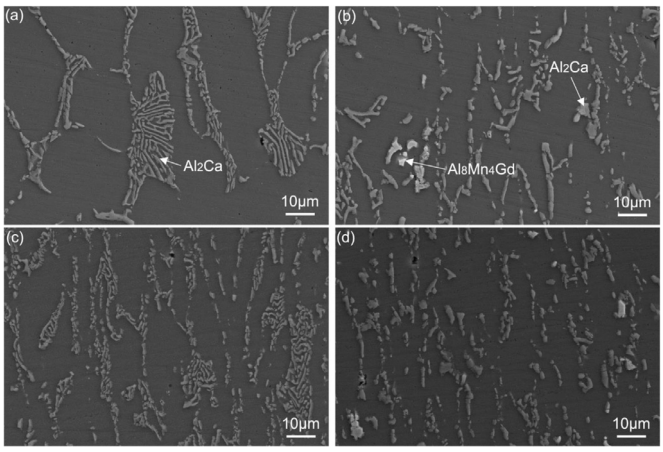

Fig. 5. The SEM morphologies of as-cast Mg-2.5Al_2Ca and Mg-2.5Al_2Ca-0.1Al_8Mn_4Gd alloys with different degree of hot rolling deformation treatment: (a and b) 50% and (c and d) 80%.

tion degree. At the same time, the distribution of Al_2Ca and Al_8Mn_4Gd particles become more uniform in Mg-2.5Al_2Ca-0.1Al_8Mn_4Gd alloy.

Fig. 6a and b show the tensile fracture of two as-cast alloys. The α-Mg dendrite form was found in tensile fracture of as-cast MgAlCa-0Gd alloy, the fracture surface was mainly occupied by cleavage surfaces. However, no α-Mg dendrite form was found in tensile fracture of as-cast MgAlCa-0.1Gd alloy, some tearing ridges occupied the fracture surface. Fig. 6c and d present the tensile fracture surfaces of hot rolled specimens with 80% deformation degree. The tear edge accompanied with dimples were found in hot rolled Mg-2.5Al_2Ca alloy, while only dimples were observed in hot rolled Mg-2.5Al_2Ca-0.1Al_8Mn_4Gd alloy. Therefore, it can be concluded that addition of Gd into Mg–Al–Ca alloys facilitate the thermal deformation (such as hot rolling) and are conductive to improve their mechanical properties.

4. Conclusions

In this study, we proved that we could regulate the microstructure of Mg–Al–Ca magnesium alloy through the formation of Al_8Mn_4Gd phase. XRD and Bramfitt's theory indicates that spherical and dispersed Al_8Mn_4Gd phase firstly precipitate during the solidification process by introduction of Mn and Gd into Mg–Al–Ca magnesium alloy, Al_8Mn_4Gd phase could efficiently restricted the growth of dendritic α-Mg and disperse lamellar Al_2Ca in Mg-2.5Al_2Ca alloy. This is because that Al_8Mn_4Gd phase can serve as heterogeneous nucleation sites for the formation of α-Mg grains and Al_2Ca particles, especially for α-Mg. In addition, the introduction of Gd into Mg–Al–Ca alloys could also facilitate the hot rolling deformation. With 50% hot-roll deformation, the UTS and ductility of as-cast Mg-2.5Al_2Ca-0.1Al_8Mn_4Gd alloy were remarkably enhanced from 140 MPa and 1.1% to be 225 MPa and 1.6%. In contrast, the UTS and elongation of Mg-2.5Al_2Ca were only enhanced from 119 MPa and 0.95% to be 140 MPa and 1.1%.

Acknowledgement

This work was financially supported by the National Science Foundation of China (No. 51701010) and by Beijing Government Funds for the Constructive Project of Central Universities (No. 353139535). Thanks to Gaomi Xiangyu Company (Shandong province, China) for the gravity casting.

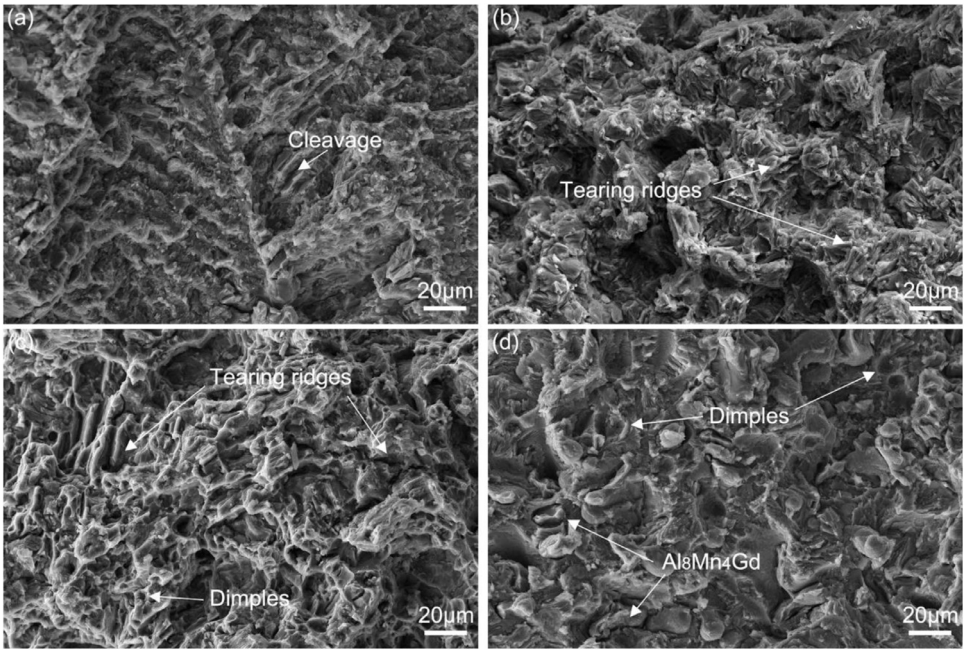

Fig.6. Fracture surface of specimens without hot roll treatment (a) and (b)and with hot rolled 80% degrees (c and d).

Please cite this article as: C. Ma, W. Yu, X. Pi et al., Study of Mg–Al–Ca magnesium alloy ameliorated with designed Al8Mn4Gd phase, Journal of Magnesium and Alloys, https://doi.org/10.1016/j.jma.2020.08.009

References

[1] F.S. Pan, M.B. Yang, X.H. Chen, A review on casting magnesium alloys: modification of commercial alloys and development of new alloys, J. Mater. Sci. Technol. 32 (2016) 1211–1221.
[2] W.J. Joost, P.E. Krajewski, Towards magnesium alloys for high-volume automotive applications, Scr. Mater. 128 (2017) 107–112.
[3] S. Otarawanna, C.M. Gourlay, H.I. Laukli, A.K. Dahle, The thickness of defect bands in high-pressure die castings, Mater. Charact. 60 (2009) 1432–1441.
[4] W.B. Yu, Y.Y. Cao, X.B. Li, Z.P. Guo, S.M. Xiong, Determination of interfacial heat transfer behavior at the metal/shot sleeve of high pressure die casting process of AZ91D alloy, J. Mater. Sci. Technol. 33 (2017) 52–58.
[5] X.B. Li, W.B. Yu, J.S. Wang, S.M. Xiong, Influence of melt flow in the gating system on microstructure and mechanical properties of high pressure die casting AZ91D magnesium alloy, Mater. Sci. Eng. -Struct. Mater. Properties Microstruct. Process. 736 (2018) 219–227.
[6] T.C. Xu, Y. Yang, X.D. Peng, J.F. Song, F.S. Pan, Overview of advancement and development trend on magnesium alloy, J. Magnes. Alloy. 7 (2019) 536–544.
[7] J.P. Weiler, A review of magnesium die-castings for closure applications, J. Magnes. Alloy. 7 (2019) 297–304.
[8] J.F. Song, J. She, D.L. Chen, F.S. Pan, Latest research advances on magnesium and magnesium alloys worldwide, J. Magnes. Alloy. 8 (2020) 1–41.
[9] Y.Z. Du, M.Y. Zheng, B.L. Jiang, Comparison of microstructure and mechanical properties of Mg-Zn microalloyed with Ca or Ce, Vacuum 151 (2018) 221–225.
[10] A.A. Luo, B.R. Powell, A.K. Sachdev, Computational phase equilibria and experimental investigation of magnesium-aluminum-calcium alloys, Intermetallics 24 (2012) 22–29.
[11] A. Suzuki, N.D. Saddock, J.W. Jones, T.M. Pollock, Solidification paths and eutectic intermetallic phases in Mg-Al-Ca ternary alloys, Acta Mater. 53 (2005) 2823–2834.
[12] H. Huang, H. Liu, C. Wang, J.P. Sun, J. Bai, F. Xue, J.H. Jiang, A.B. Ma, Potential of multi-pass ECAP on improving the mechanical properties of a high-calcium-content Mg-Al-Ca-Mn alloy, J. Magnes. Alloy. 7 (2019) 617–627.
[13] Q. Yang, F.Q. Bu, T. Zheng, F.Z. Meng, X.J. Liu, D.P. Zhang, X. Qiu, J. Meng, Influence of trace Sr additions on the microstructures and the mechanical properties of Mg-Al-La-based alloy, Mater. Sci. Eng. -Struct. Mater. Properties Microstruct. Process. 619 (2014) 256–264.
[14] Q. Yang, T. Zheng, D.P. Zhang, X.J. Liu, J. Fan, X. Qiu, X.D. Niu, J. Meng, Microstructures and tensile properties of Mg-4Al-4La-0.4Mn-xB (x=0, 0.01, 0.02, 0.03) alloy, J. Alloy. Compd. 572 (2013) 129–136.
[15] L.W. Zheng, H.H. Nie, W.G. Zhang, W. Liang, Y.D. Wang, Microstructural refinement and improvement of mechanical properties of hot-rolled Mg-3Al-Zn alloy sheets subjected to pre-extrusion and Al-Si alloying, Mater. Sci. Eng. -Struct. Mater. Properties Microstruct. Process. 722 (2018) 58–68.
[16] Q. Yang, K. Guan, F.Q. Bu, Y.Q. Zhang, X. Qiu, T. Zheng, X.J. Liu, J. Meng, Microstructures and tensile properties of a high-strength die-cast Mg-4Al-2RE-2Ca-0.3Mn alloy, Mater. Charact. 113 (2016) 180–188.
[17] Z.T. Li, X.G. Qiao, C. Xu, X.Q. Liu, S. Kamado, M.Y. Zheng, Enhanced strength by precipitate modification in wrought Mg-Al-Ca alloy with trace Mn addition, J. Alloy. Compd. (2020) 154689.
[18] T. Nakata, C. Xu, K. Suzawa, K. Yoshida, N. Kawabe, S. Kamado, Enhancing mechanical properties of rolled Mg-Al-Ca-Mn alloy sheet by Zn addition, Mater. Sci. Eng. 737 (2018) 223–229.
[19] H.-.T. Son, J.-.S. Lee, D.-.G. Kim, K. Yoshimi, K. Maruyama, Effects of samarium (Sm) additions on the microstructure and mechanical properties of as-cast and hot-extruded Mg-5wt%Al-3wt%Ca-based alloys, J. Alloy. Compd. 473 (2009) 446–452.
[20] J. Wang, X. Li, Simultaneously improving strength and ductility of AZ91-type alloys with minor Gd addition, J. Alloy. Compd. 803 (2019) 689–699.
[21] B.L. Bramfitt, Effect of carbide and nitride additions on heterogeneous nucleation behavior of liquid iron, Metall. Trans. 1 (1970) 1987.
[22] M.X. Zhang, P.M. Kelly, M. Qian, J.A. Taylor, Crystallography of grain refinement in Mg-Al based alloys, Acta Mater. 53 (2005) 3261–3270.
[23] Y. Ali, D. Qiu, B. Jiang, F. Pan, M.-.X. Zhang, Current research progress in grain refinement of cast magnesium alloys: a review article, J. Alloy. Compd. 619 (2015) 639–651.
[24] M. Han, X. Zhu, T. Gao, X. Liu, Revealing the roles of Al4C3 and Al8Mn5 during α-Mg nucleation in Mg-Al based alloys, J. Alloy. Compd. 705 (2017) 14–21.
[25] Y. Wang, M. Xia, Z. Fan, X. Zhou, G.E. Thompson, The effect of Al8Mn5 intermetallic particles on grain size of as-cast Mg-Al-Zn AZ91D alloy, Intermetallics 18 (2010) 1683–1689.

Please cite this article as: C. Ma, W. Yu, X. Pi et al., Study of Mg–Al–Ca magnesium alloy ameliorated with designed Al8Mn4Gd phase, Journal of Magnesium and Alloys, https://doi.org/10.1016/j.jma.2020.08.009